Kinetic and Thermodynamic Analysis on OH Addition to Ethylene: Adduct Formation, Isomerization, and Isomer Dissociations

Takahiro Yamada, Joseph W. Bozzelli,* and Tsan Lay

Department of Chemical Engineering, Chemistry, and Environmental Science, New Jersey Institute of Technology, Newark, New Jersey 07102

Received: January 15, 1999; In Final Form: May 28, 1999

Reaction pathways and kinetics are analyzed as function of temperature and pressure on formation and reactions of the adduct resulting from OH addition to ethylene. Ab initio methods are used to determine thermodynamic properties of intermediate radicals, transition states (TS) and vinyl alcohol. Enthalpies of formation ($\Delta H_f^\circ{}_{298}$ in kcal/mol) are determined for $C\cdot H_2CH_2OH$, $CH_3CH_2O\cdot$, and CH_2CHOH using CBS-q//MP2(full)/6-31G(d,p) and G2 methods with isodesmic reactions, where zero point vibrational energies (ZPVE) and thermal correction to 298.15 K are incorporated. $\Delta H_f^\circ{}_{298}$ of TS's are determined for $C\cdot H_2CH_2OH$ (H atom shift), CH_3CHO-H (β-scission to form acetaldehyde + H), CH_3-CH_2O (β-scission to form formaldehyde + methyl radical) and $CH_2CHOH-H$ (β-scission to form vinyl alcohol + H) using CBS-q//MP2(full)/6-31G(d,p) and G2 methods. Entropies (S°_{298} in cal/mol K) and heat capacities ($C_p(T)$ $300 \le T/K \le 1500$ in cal/mol K) are determined using geometric parameters and scaled vibrational frequencies obtained at the MP2(full)/6-31G(d,p) level of theory for CBS-q calculations. Geometric parameters obtained at MP2(full)/6-31G(d) level of theory and vibrational frequencies obtained at HF/6-31G(d) are used for G2 calculations. Quantum Rice−Ramsperger−Kassel (QRRK) analysis is used to calculate energy dependent rate constants, $k(E)$, and master equation analysis is used to account for collisional stabilization. Rate constants are compared with experimentally determined product branching ratios ($C\cdot H_2CH_2OH$ stabilization: $CH_2O + CH_3$:$CH_3CHO + H$). OH adds to ethylene to form an energized ethylene-OH adduct radical ($C\cdot H_2CH_2OH$)*. This energized adduct can dissociate back to reactants, isomerize via hydrogen shift ($E_{a,rxn} = 29.8$ and 30.8 kcal/mol) to form CH_3CH_2O, ($\Delta H_f^\circ{}_{298} = -1.7$ and -3.3 kcal/mol) for CBS-q and G2 calculations respectively, or be stabilized. The $CH_3CH_2O\cdot$ isomer can undergo β-scission reaction to either formaldehyde (CH_2O) + methyl radical (CH_3) ($E_{a,rxn} = 13.4$ and 16.0 kcal/mol) or acetaldehyde CH_3CHO + H atom ($E_{a,rxn} = 17.6$ and 19.2 kcal/mol) for CBS-q and G2 calculations, respectively. Hydrogen atom tunneling is included by use of the Eckart formalism. Tunneling effect coefficients are 842, 93.1, and 21.1 for $C\cdot H_2CH_2OH \rightarrow CH_3CH_2O$, $CH_3CH_2O\cdot \rightarrow C\cdot H_2CH_2OH$ and $CH_3CH_2O\cdot \rightarrow CH_3CHO + H$ at 295 K, respectively. Chemical activation and falloff are determined to be of major importance in determination of the dominant reaction paths and rate constants versus pressure and temperature in this three heavy atom system.

Introduction

The OH addition to ethylene is important in mid temperature hydrocarbon combustion chemistry (below 1200 K) and in tropospheric photochemistry. The C−H bond energy in ethylene is 111.6 kcal/mol and abstraction of this H by the OH radical has an activation energy of ca. 7 kcal/mol, while the addition of OH radical to the Π bond has zero or negative activation energy and a similar preexponential factor.[1−6] The adduct is a small molecule, three heavy atoms, and the reactions exhibit significant pressure dependence, falloff, with temperature. This addition is the dominant reaction path below 1000 K and kinetic values are needed for the reaction channels as a function of pressure and temperature. The energized adduct formed by the addition can undergo elimination to a new product set vinyl alcohol + H, reverse reaction, isomerize, and react to new products, or the isomers can be stabilized. Vinyl alcohol has a weak O−H bond (ca. 85 kcal/mol); it rapidly undergoes abstraction to form formyl-methyl radical (loss of the O−H hydrogen then electron rearrangement to formyl-methyl radical ($C\cdot H_2CHO$). Other product sets, $CH_3 + CH_2O$ and CH_3CHO + H, have been observed as important channels under low-pressure conditions. Kinetic data for these channels as a function of temperature and pressure have not been previously evaluated nor are the vinyl alcohol or aldehyde product sets included in atmospheric or combustion models. We evaluate pathways and rate constants for these reaction processes over a wide range of temperature and pressure in this study and estimate rate constants for use in combustion and atmospheric kinetic modeling. Chemical activation and falloff are of major importance in determination of the primary reaction paths and their rate constants versus pressure and temperature in this small molecule, three heavy atom system.

Several ab initio studies[1,7−9] have been performed on the addition−isomerization reaction system and kinetics (mostly on OH loss) from a number of experimental studies[2−6,10−23] are available for comparison. There are, however, limited kinetic studies utilizing the ab initio thermodynamic properties or

10.1021/jp990193g CCC: $18.00
Published on Web 09/03/1999

thermochemical kinetic data for evaluation of reaction paths and product sets versus temperature and pressure.

Sosa et al. calculated barrier heights for C_2H_4 + OH using Unrestricted Møller−Plesset Perturbation Theory with spin annihilation.[1] They also studied reaction pathways for adduct ($C\cdot H_2CH_2OH$) reaction to products using geometries optimized at HF/6-31G* and energy of up to MP4SDQ/6-31G** levels of calculations.

Villa et al. studied the activation energy and rate constant trends for C_2H_4 + OH addition to form $C\cdot H_2CH_2OH$ using canonical variational transition state theory and reaction potential-energy hypersurface using several ab initio methods.[7] Their calculations demonstrate a strong inverse dependence of the rate constant with temperature under 565 K, in agreement with the experimental evidence that this reaction has a negative activation energy at atmospheric temperatures.

Liu et al. studied the reaction using high temperature gas phase pulse radiolysis to determine the rate of the reaction and report a weak negative activation energy (−0.95 kcal/mol) below 560 K.[13] Atkinson et al. reported absolute rate constants for the reaction of OH radical with ethylene using flash photolysis−resonance fluorescence technique and indicates that rate constants are independent of total pressure over the range 255−663 torr.[4]

Bartels et al.[12] studied the OH plus ethylene reaction at temperature of 295 K and low pressure (0.1−2 torr) using discharge flow and laval nozzle reactors with molecular beam mass spectrometric detection. They reported branching ratios at 295 K and 2 torr for $C\cdot H_2CH_2OH$ stabilization, CH_2O + CH_3 and CH_3CHO + H determined by direct calibration procedures. They ascribe the reaction pathways as resulting from chemical activation.

Fulle et al.[23] studied fall-off in 1 to 139 Bar He by OH fluorescence and report a high pressure rate constant of 6E12 between 300 and 800 K. They interpret the adduct as having no exit channels, but point out that reliable data for new product channel barriers is not available.

Orlando et al. analyzed this reaction system relevant to atmospheric conditions; they report that the $OH-C_2H_4$ adduct rapidly reacts with O_2 to form peroxy radical which then undergoes chemical activation reaction with NO to yield an energized alkoxy radical plus NO_2.[51] The energized alkoxy dissociates to several product sets before collisional stabilization. Their calculation indicates hydrogen bonding between the alcohol H atom and the alkoxy oxygen provide added well depth of ca. 2 kcal/mol which is needed to explain the chemical activation reaction results.

In this work, thermodynamic properties ($\Delta H_f°_{298}$, $S°_{298}$, and $C_p(T)$'s, 300 → T/K → 1500) of intermediate radicals $C\cdot H_2CH_2$-OH and $CH_3CH_2O^\bullet$, product CH_2CHOH and of the following transition states: (TS1) $C\cdot H_2CH_2OH$, intramolecular hydrogen shift to form $CH_3CH_2O^\bullet$, (TS2) CH_3-CH_2O, β-scission reaction to form methyl radical plus formaldehyde, (TS3) CH_3CHO-H, β-scission reaction to form acetaldehyde plus atomic hydrogen, (TS4) C·H2CHOH−H, β-scission reaction to form vinyl alcohol plus atomic hydrogen, are calculated using CBS-q[25] and G2[26] composite methods in the Gaussian94 computer code.[27] Isodesmic reactions are applied to estimate $\Delta H_f°_{298}$ of two intermediate radicals, $C\cdot H_2CH_2OH$ and $CH_3CH_2O^\bullet$ and product CH_2CHOH; data are compared to literature where available. The calculated activation energies of four TS's are compared with estimated values of Bartels et al.[12] and previous ab initio determined reaction pathway analysis.[8] CBS-q[25]// MP2(full)/6-31G(d,p) determined thermodynamic properties are chosen for the detailed kinetic analysis.

Quantum Rice−Ramsperger−Kassel (QRRK) analysis[23,24] is used to calculate the energy dependent rate constants $k(E)$, and master equation analysis is applied to account for collisional stabilization in the C_2H_4 + OH adduct and isomers.

Comparisons of the calculated branching ratio ($C\cdot H_2CH_2OH$ stabilization: CH_2O+CH_3:CH_3CHO+H) at 2 torr and 295 K with the experimentally determined ratio suggests the need to invoke tunneling for the hydrogen shift transition state (TS1) $C\cdot H_2CH_2OH^\bullet \rightleftarrows CH_3CH_2O^\bullet$ and for the H atom elimination (β-scission) transition state (TS3) $CH_3CH_2O^\bullet \rightarrow CH_3CHO$ + H. Imaginary frequencies obtained at MP2(full)/6-31G(d,p) level of theory need to be adjusted downward to match the experimentally determined branching ratio with a chemical activation reaction analysis on the $(C\cdot H_2CH_2OH)^*$ adduct when tunneling is included.

Method

G2 theory is based on MP2(full)/6-31G(d) optimized geometry and HF/6-31G(d) determined vibrational frequencies. G2 theory uses the 6-311G(d,p) basis set and correlation's for several basis set extensions. Treatment of correlation is by Møller−Plesset (MP) perturbation theory and quadratic configuration interaction (QCISD). The final total energies obtained in G2 theory are effectively at the QCISD(T)/6-311G+G(3df, 2p) level, allowing for certain assumptions about additivity of the correlation.[26] Transition state geometries are identified by the existence of one imaginary frequency in the normal mode coordinate analysis, analysis of its structure and vibration motion.

The CBS-q calculation sequence in this study is performed on the geometry and frequencies determined by a MP2(full)/6-31G(d,p) calculation; HF/3-21 G(d) is the suggested method for structure and frequency calculation with CBS-q. This MP2 calculation is followed by a self-consistent field energy calculation HF/CBS1, a second-order calculation of MP2/6-31+D**. Pair coupling effects from polarization functions and spin contamination in open shell molecules are treated with MP4/(SDQ)/6-31g(D') and QCISD(T)/6-31G levels of theory, respectively.[25]

We choose MP2(full)/6-31G(d,p) for the geometry optimization because it is consistent with G2; higher level calculations may result in more accurate structures and energies.

1. Entropies and Heat Capacities. $S°_{298}$ and $C_p(T)$s are calculated based on scaled frequencies and moments of inertia of the optimized MP2(full)/6-31G(d,p) geometry for CBS-q method, and scaled frequencies of the optimized HF/6-31G(d) geometry and moments of inertia of the optimized MP2(full)/6-31G(d) geometry for G2 method. The vibrational scaling factors are 1.0232 for MP2(full)/6-31G(d,p)[29] and 0.8929 for HF/6-31G(d) calculation.[30] ab initio calculated internal rotational frequencies are not included for $S°_{298}$ and $C_p(T)$'s calculations. Contribution of internal rotational to $S°_{298}$ and $C_p(T)$'s are calculated separately based on rotational barrier height and moments of inertia. Pitzer et al.'s[31] general treatment of internal rotation is used to calculate the hindered internal rotational contribution to $S°_{298}$ and $C_p(T)$'s: data are presented in Table 5 (below). $S°_{298}$'s and $C_p(T)$'s for reactants and other products are obtained from literature.[32,33]

2. Determination of Enthalpies of Formation. $\Delta H_f°_{298}$ for two intermediate radicals and the product are estimated using total energies obtained by ab initio calculations and the following

isodesmic reactions:

$$C\cdot H_2CH_2OH + C_2H_6 \rightarrow CH_3CH_2OH + C_2H_5$$

(1) for estimation of $C\cdot H_2CH_2OH$

$$CH_3CH_2O^\bullet + CH_3OH \rightarrow CH_3CH_2OH + CH_3O^\bullet$$

(2) for estimation of $CH_3CH_2O^\bullet$

$$CH_2CHOH + CH_3CH_3 \rightarrow CH_2CH_2 + CH_3CH_2OH$$

(3) for estimation of vinyl alcohol.

The method of isodesmic reactions relies upon the similarity of bonding environment in the reactants and products that leads to cancelation of systematic errors in the ab initio MO calculations.[30] An isodesmic reaction requires bond type conservation; the number of each chemical bond type must be conserved in the reaction. An isodesmic reaction will lead to more accurate enthalpy estimations if groups are also conserved; group conservation allows correlation of next-nearest-neighbor atoms in reactants and products, in addition to bond types.[34] Reactions 1 and 2 conserve both bond and group types. Ab initio calculations with ZPVE and thermal correction are performed for all of four compounds in reaction 1. The unknown $\Delta H_f^\circ{}_{298}$ of $C\cdot H_2CH_2OH$ is obtained from the calculated ($H_{rxn}^\circ{}_{298}$ and the experimentally or theoretically determined $\Delta H_f^\circ{}_{298}$ of three other compounds in eq 1. The analogous values for $CH_3CH_2O^\bullet$ and product C_2H_3OH are calculated in the same manner.

Values of $\Delta H_f^\circ{}_{298}$ for reactants and products (except vinyl alcohol) are obtained from literature.[32,33] Use of calculated values and isodesmic reactions with group balance for determination of these enthalpies would result in values within 1 kcal/mol or less of the literature, because literature values are used for the species in the isodesmic reactions. Further discussion is presented below.

Total energies are corrected by ZPVE which are scaled by 0.9608 as recommended by Scott et al.[29] for MP2(full)/6-31G(d,p) and 0.8929 for HF/6-31G(d).[30] Thermal correction 0−298.15K is calculated to estimate enthalpy of formation at 298.15 K using the following equations:[30]

$$\Delta H(T) = H_{trans}(T) + H_{rot}(T) + \Delta H_{vib}(T) + RT \quad (1)$$

$$H_{trans}(T) = 3/2RT$$

$$H_{rot}(T) = 3/2RT \quad (2)$$

$$\Delta H_{vib}(T) = Nh\Sigma(\nu_i/(\exp(h\nu_i/k_bT) - 1)) \quad (3)$$

where N, h, and k_b are the Avogadro constant, Plank constant, and Boltzman constants, respectively. The ν_i's are scaled by 1.0084 for MP2(full)/6-31G(d,p)[29] and 0.8929 for HF/6-31G-(d) as recommended by Hehre.[30]

$\Delta H_f^\circ{}_{298}$ of TS compounds are estimated by evaluation of $\Delta H_f^\circ{}_{298}$ of the stable intermediate radicals plus difference of total energies with ZPVE and thermal correction between these radical species and the TSs.

3. High-Pressure Limit A factors (A_∞) and Rate Constant (k_∞) Determination with *ab Initio* Calculations for Transition State Compounds. For the reactions where thermodynamic properties of transition states are calculated by ab initio methods, k_∞'s are expressed by

$$k_\infty = A_\infty(T)^n\exp(-E_{a,\infty}/RT) \quad (4)$$

The high-pressure limit A factors ($A_($) of unimolecular reactions are calculated using conventional transition state theory (TST).[35] Loss (or gain) of internal rotors and change of optical isomer and symmetry numbers are incorporated into the calculation of S°_{298} for each TS. S°_{298}'s of reactants and TSs are then used to determine the preexponential factor A via TST[35] for a unimolecular reaction

$$A = (k_bT/h_p)\exp(\Delta S^{\neq}) \quad (5)$$

where h_p is Plank's constant, k_b is the Boltzmann constant, and $\Delta S^{\neq}$ is equal to $S^\circ_{298,TS} - S^\circ_{298,reactant}$.

Activation energies of reactions are calculated as follows:

$$E_a = \{\Delta H_f^\circ{}_{298,TS} - \Delta H_f^\circ{}_{298,reactant}\} \quad (6)$$

4. Quantum Rice−Ramsperger−Kassel (QRRK) Analysis with Master Equation. Unimolecular dissociation and isomerization reactions of the chemically activated and stabilized adducts resulting from addition or combination reactions are analyzed by first constructing potential energy diagrams. Thermodynamic parameters, $\Delta H_f^\circ{}_{298}$, S°_{298}, and $C_p(T)$'s 300 → T/K (1500), reduced vibration frequency sets, and Lennard Jones parameters for species in each reaction path are presented.

The high-pressure rate constants for each channel are obtained from literature or reference material. The high-pressure limit rate constant (k_∞) for $C_2H_4 + OH \rightarrow C\cdot H_2CH_2OH$ is taken from recently published theoretically derived values.[7] Their values are derived using canonical variational transition state theory and they vary nonlinearly with temperature. The reverse rate constants are estimated from the principles of microscopic reversibility (MR). Kinetic parameters for unimolecular and bimolecular (chemical activation) reactions are then calculated using multifrequency QRRK analysis for $k(E)$.[36−38] The master equation analysis,[37] as described by Gilbert and Smith,[39] and in their *UNIMOL* code manual,[40] is used for falloff with the steady state assumption on the energized adduct(s).

5. Tunneling Effect and Experimental Data Comparison. Tunneling is applied for the intramolecular hydrogen atom transfer reaction of TS1 and hydrogen atom dissociation reaction TS3, since the direct calculation results of branching ratios ($C\cdot H_2CH_2OH$ stabilization:$CH_2O + CH_3$:$CH_3CHO + H$) do not show good agreement with experimental values. CBS-q energies are chosen for use in the kinetic analysis for consistency. G2 enthalpies are slightly higher for H atom transfer in TS1 plus in TS2 and TS3, the two aldehyde products, and require a slightly larger, but not unreasonable, adjustment to fit the data.

Tunneling effects are taken into account using the Erwin−Henry computer code[41] to determine high-pressure limit rate constants (k_∞) of reactions 2 and 4. This program is based on Eckart's one-dimensional potential function.[42] Eckart evaluated in closed form, an expression for the probability κ(E) of crossing the barrier for a particle of energy E. The Erwin−Henry computer code requires input of vibrational frequencies, moments of inertia and total energies at 0 K of reactants, transition states, and products; imaginary frequencies are also required. Total energies are obtained from the CBS-q methods, vibrational frequencies and moments of inertia are obtained from MP2(full)/6-31G(d,p) level of calculation.

Imaginary frequencies are adjusted to fit the experimentally derived branching ratio, as in William et al[46] since the direct use of imaginary frequencies from HF or MP2(full)/6-31G(d,p) is reported to give unreasonably high correction factors Γ*. The Γ* are calculated with the adjusted imaginary frequencies at

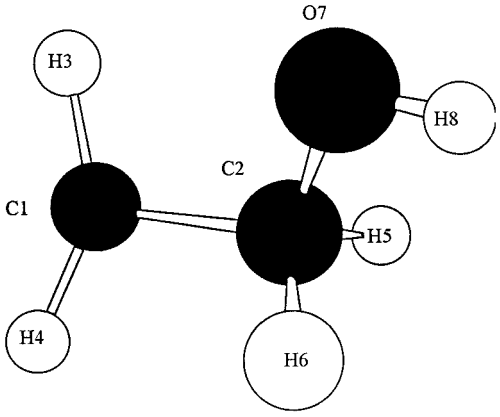

Description	MP2(full)/6-31G(d,p)	MP2(full)/6-31G(d)
C2-C1	1.482	1.483
H3-C1	1.077	1.082
H4-C1	1.076	1.081
H5-C2	1.100	1.105
H6-C2	1.096	1.101
O7-C2	1.425	1.427
H8-O7	0.963	0.971
∠3,1,2	120.1	120.3
∠4,1,2	118.9	119.0
∠5,2,1	110.4	110.5
∠6,2,1	110.0	110.1
∠7,2,1	108.1	107.9
∠8,7,2	107.4	107.5

Figure 1. Geometry of $C{\cdot}H_2CH_2OH$.

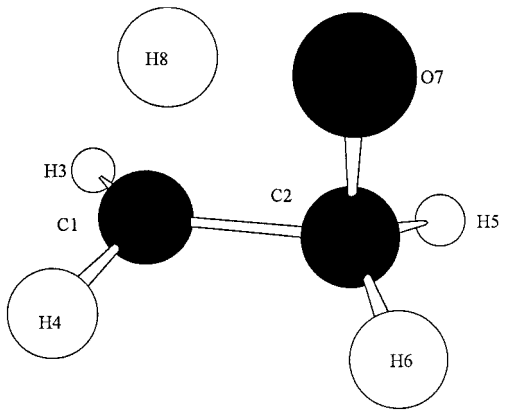

Description	MP2(full)/6-31G(d,p)	MP2(full)/6-31G(d)
C2-C1	1.495	1.495
H3-C1	1.081	1.086
H4-C1	1.081	1.086
H8-C1	1.306	1.332
H5-C2	1.088	1.093
H6-C2	1.088	1.093
O7-C2	1.446	1.449
H8-O7	1.250	1.249
∠3,1,2	117.8	118.0
∠4,1,2	117.8	118.0
∠5,2,1	115.9	115.9
∠6,2,1	115.9	116.0
∠8,1,2	81.0	81.1
∠7,2,1	88.0	88.2
∠7,8,1	104.3	105.0
∠8,7,2	84.9	85.7

Figure 2. Geometry of TS1 $C{\cdot}H_2CH_2OH$.

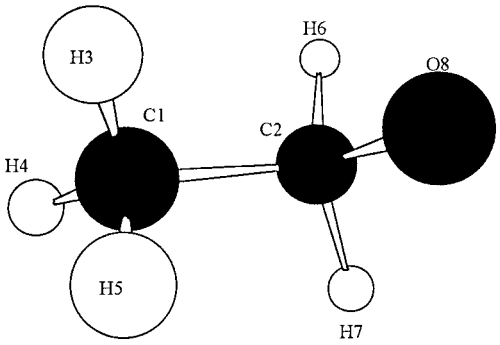

Description	MP2(full)/6-31G(d,p)	MP2(full)/6-31G(d)
C2-C1	1.531	1.533
H3-C1	1.086	1.091
H4-C1	1.087	1.093
H5-C1	1.086	1.091
O8-C2	1.389	1.390
H6-C2	1.093	1.098
H8-C2	1.093	1.098
∠3,1,2	110.3	110.3
∠4,1,2	109.2	109.3
∠5,1,2	110.3	110.3
∠8,2,1	106.1	106.0
∠7,2,1	109.5	109.6
∠6,2,1	109.5	109.6

Figure 3. Geometry of CH_3CH_2O.

temperatures, 290, 295, 325, 400, 524, 700, 900, and 1200 K. These numbers are convolved into the A_∞ values determined from TST.

Results and Discussion

1. Geometries and Frequencies. Figures 1−6 show optimized geometries of two intermediate radicals and four TS compounds by MP2(full)/6-31G(d,p) and MP2(full)/6-31G(d) calculations. The two methods give similar results: geometric parameters from the higher theory, MP2(full)/6-31G(d,p), are listed unless otherwise noted. Tables 1 and 2 list the frequency calculation results of MP2(full)/6-31G(d,p) and HF/6-31G(d).

The C_2-C_1 bond length in TS1, H shift from the hydroxyl to the methyl, is 1.495 Å, which is slightly longer than C_2-C_1 bond length of reactant ($C{\cdot}H_2CH_2OH$), 1.482 Å, and shorter than C_2-C_1 bond length of product ($CH_3CH_2O^{\bullet}$), 1.531 Å. The O_7-C_2 bond length is slightly stretched (1.446 Å) in TS1 (ca. 0.02 Å) then shortened to 1.389 Å in the product $CH_3CH_2O^{\bullet}$. The bond length of H_8-O_7, which is 0.963 Å, in the reactant is stretched to 1.250 Å in TS1. The H_8-C_1 bond forming is 1.306 Å at TS1. The imaginary frequencies at TS1 are 2344i and 2909i cm^{-1} for MP2(full)/6-31G(d,p) and HF/6-31G(d) levels of theory, respectively.

Figure 4 shows the TS2 geometry, β-scission of $CH_3CH_2O^{\bullet} \rightarrow CH_3 + CH_2O$. The bond length of C_2-C_1 in TS2 is 2.071 Å, which is 1.531 Å in $CH_3CH_2O^{\bullet}$. The O_6-C_2 bond length also changes from 1.389 to 1.220 Å, indicative of the CO double bond formation in TS2 (bond length of the formaldehyde C═O double bond is 1.219 Å at the same level of theory). The imaginary frequencies at TS2 are 685i and 550i cm^{-1} for MP2(full)/6-31G(d,p) and HF/6-31G(d) level of theory, respectively.

The H_8-C_2 bond length is 1.622 Å, and O_6-C_2 is 1.220 Å at TS3 in Figure 5, which is same as the C−O bond length of

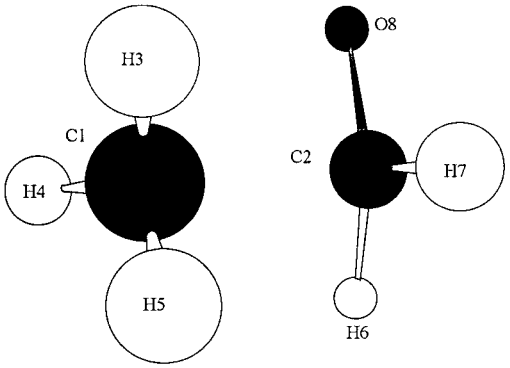

Description	MP2(full)/6-31G(d,p)	MP2(full)/6-31G(d)
C2-C1	2.071	2.071
H3-C1	1.080	1.080
H4-C1	1.077	1.081
H5-C1	1.077	1.081
O8-C2	1.220	1.220
H7-C2	1.102	1.102
H6-C2	1.102	1.102
∠3,1,2	100.9	101.1
∠4,1,2	100.2	100.1
∠5,1,2	100.2	100.1
∠8,2,1	102.9	102.7
∠7,2,1	91.1	91.3
∠6,2,1	91.0	91.3

Figure 4. Geometry of TS2 CH_3-CH_2O.

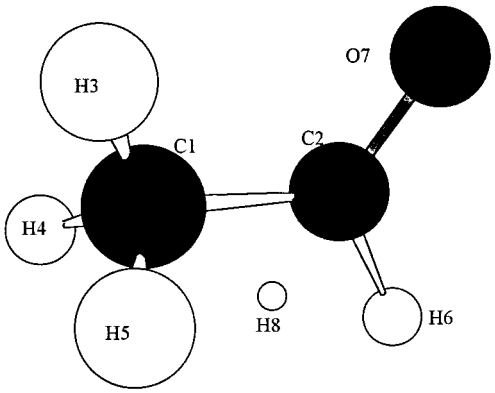

Description	MP2(full)/6-31G(d,p)	MP2(full)/6-31G(d)
C1-C2	1.512	1.514
H3-C1	1.090	1.095
H4-C1	1.085	1.090
H5-C1	1.087	1.092
O7-C2	1.220	1.225
H6-C2	1.107	1.111
H8-C2	1.622	1.600
∠3,1,2	107.1	107.3
∠4,1,2	109.9	109.8
∠5,1,2	112.0	112.1
∠7,2,1	123.0	122.7
∠6,2,1	114.6	114.8
∠8,2,1	98.3	98.7

Figure 5. Geometry of TS3 $CH_3CHO\cdots H$.

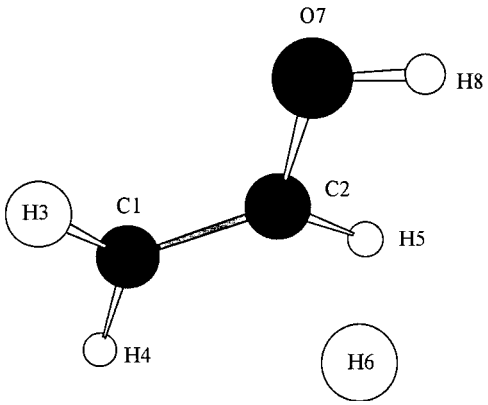

Bond Angle (degree)	MP2(full)/6-31G(d,p)	MP2(full)/6-31G(d)
C1-C2	1.340	1.345
H3-C1	1.076	1.081
H4-C1	1.077	1.082
H5-C2	1.083	1.088
H6-C2	1.795	1.772
O7-C2	1.371	1.376
H8-O7	0.963	0.971
∠3,1,2	119.9	120.1
∠4,1,2	120.6	12.07
∠5,2,1	120.9	120.8
∠6,2,1	99.4	100.5
∠7,2,1	120.1	119.5
∠8,2,1	108.6	108.6

Figure 6. Geometry of TS4 $CH_2CHOH\cdots H$.

TABLE 1: Vibrational Frequencies[a] (ν cm^{-1}) MP2(full)/6-31G(d,p) Level of Calculation

species	ν1[c]	ν2	ν3	ν4	ν5	ν6	ν7	ν8	ν9	ν10	ν11	ν12	ν13	ν14	ν15	ν16	ν17	ν18
$C\cdot H_2CH_2OH$	181	293	411	473	898	1011	1113	1154	1259	1301	1479	1532	1572	3025	3088	3277	3402	3902
$C\cdot H_2CH_2OH$ (TS1)[b]	2344i	383	767	854	968	1041	1136	1159	1180	1265	1332	1490	1595	2115	3152	3221	3227	3350
$CH_3CH_2O^{\bullet}$	266	396	673	932	988	1027	1172	1303	1376	1449	1545	1565	1608	3094	3152	3156	3257	3265
CH_3-$CH_2O^{\bullet}$ (TS2)[b]	685i	180	319	587	641	736	972	1207	1303	1489	1508	1572	1737	2990	3059	3207	3386	3406
CH_3CHO-H (TS3)[b]	1704i	222	488	563	622	883	958	1155	1227	1435	1460	1534	1541	1771	2979	3141	3238	3276
$CH_2CH(OH)$-H (TS4)[b]	1318i	297	472	546	555	730	887	984	1121	1186	1304	1362	1491	1694	3251	3288	3403	3913
CH_2CHOH	466	494	722	805	981	1012	1142	1355	1388	1496	1749	3258	3301	3373	3868			

[a] Non-scaled. [b] TS structure described in Method section. [c] Transition state compounds have one imaginary frequency.

TS2. The bond length of C_2-C_1 is slightly shorter (ca. 0.02 Å) than that of reactant $CH_3CH_2O^{\bullet}$. The imaginary frequencies are 1704i and 1118i cm^{-1} for MP2(full)/6-31G(d,p) and HF/6-31G(d) level of theory, respectively.

Figure 6 shows the TS4 geometry, β-scission of $C\cdot H_2CH_2$-OH → CH_2CHOH + H. The C_2-H_6 bond length is 1.795 and 1.772 Å with MP2(full)/6-31G(d,p) and MP2(full)/6-31g(d) calculations, respectively, slightly large difference between two calculations. The C_1-C_2 bond length is 1.340 Å with MP2(full)/6-31G(d,p) calculation, almost forming a C−C double bond. The O_7-C_2 bond length, which is 1.371 Å, is slightly longer than the normal O−C bond length. The imaginary frequencies

TABLE 2: Vibrational Frequencies[a] (ν cm^{-1}) HF/6-31G(d) Level of Calculation

species	ν1[c]	ν2	ν3	ν4	ν5	ν6	ν7	ν8	ν9	ν10	ν11	ν12	ν13	ν14	ν15	ν16	ν17	ν18
C·H$_2$CH$_2$OH	172	301	418	481	948	1057	1158	1224	1359	1393	1565	1620	1668	3123	3174	3328	3437	4117
C·H$_2$CH$_2$OH (TS1)[b]	2909i	400	729	883	1038	1055	1162	1165	1272	1332	1452	1577	1683	1922	3249	3300	3313	3416
CH$_3$CH$_2$O·	261	425	452	973	974	1098	1239	1375	1497	1552	1627	1644	1692	3201	3221	3240	3293	3300
CH$_3$−CH$_2$O· (TS2)[b]	550i	142	295	571	656	786	949	1157	1347	1486	1562	1574	1699	3204	3269	3291	3415	3433
CH$_3$CHO−H (TS3)[b]	1118i	201	493	552	600	938	1001	1192	1224	1490	1553	1608	1622	1655	3204	3218	3275	3315
CH$_2$CH(OH)−H (TS4)[b]	843i	290	463	494	530	674	829	1023	1035	1213	1361	1419	1567	1692	3349	3361	3450	4128
CH$_2$CHOH	459	533	785	965	1048	1129	1234	1447	1468	1595	1878	3333	3402	3433	4096			

[a] Nonscaled. [b] TS structure described in Method section. [c] Transition State compounds have one imaginary frequency.

TABLE 3: List of Total Energy, ZPVE, and Thermal Correction of CBS-q Calculation[a]

	total energy at 0 K[b]	ZPVE[c]	thermal correction[d]	total energy at 298 K
C·H$_2$CH$_2$OH	−154.160 422 8	0.066 913	0.005 493	−154.154 93
C$_2$H$_5$OH	−154.826 419 7	0.082 68	0.005 141 2	−154.821 28
C$_2$H$_6$	−79.684 5026 7	0.077 584	0.004 357 9	−79.680 145
C$_2$H$_5$	−79.017 8910 9	0.061 82	0.004 777 1	−79.013 114
C·H$_2$CH$_2$OH (TS1)[e]	−154.113 929 3	0.064 325	0.004 40 68	−154.109 52
C$_2$H$_5$O·	−154.153 760 8	0.070 772	0.004 837 3	−154.148 92
CH$_3$OH	−115.576 770 1	0.053 033	0.004 222 2	−115.572 55
CH$_3$O·	−114.907 859 4	0.038 596	0.003 912 3	−114.903 95
CH$_3$−CH$_2$O· (TS2)[e]	−154.132 483 8	0.064 471	0.005 238 1	−154.127 25
CH$_3$CHO−H (TS3)[e]	−154.125 707 7	0.060 353	0.005 008 5	−154.1207
C$_2$H$_3$OH−H (TS4)[e]	−154.105 94 6	0.060 333	0.005 069 4	−154.100 88
C$_2$H$_3$OH	−153.615 472 5	0.057 89	0.004 540 8	−153.610 93
C$_2$H$_4$	−78.455 886 67	0.052 411	0.003 971	−78.451 916

[a] Unit in hartree. 1 hartree = 627.51 kcal/mol. [b] Scaled ZPVE are included. Scaling factor is recommended as 0.9608 by Scott et al.[29] [c] Nonscaled. [d] Scaled by 1.0084, Scott et al.[29] [e] TS structure described in Method section.

TABLE 4: List of Total Energy of G2 Calculation[a]

	total energy at 298 K
C·H$_2$CH$_2$OH	−154.095 490
C$_2$H$_5$OH	−154.759 163
C$_2$H$_6$	−79.626 402 0
C$_2$H$_5$	−78.965 224 0
C·H$_2$CH$_2$OH (TS1)[b]	−154.046 264 5
C$_2$H$_5$O·	−154.091 040 0
CH$_3$OH	−115.530 600 0
CH$_3$O·	−114.863 592 0
CH$_3$−CH$_2$O· (TS2)[b]	−154.065 483 8
CH$_3$CHO−H (TS3)[b]	−154.060 410 2
C$_2$H$_3$OH-H (TS4)[b]	−154.044 523 6
C$_2$H$_3$OH	−153.554 381 0
C$_2$H$_4$	−78.411 923 0

[a] Scaled ZPVE and Thermal correction 0 K to 298.15 K are taken into account. Unit in Hartree 1 Hartree = 627.51 kcal/mol. [b,c,d,e] TS structure described in Method section.

are 1318i and 843i cm^{-1} for MP2(full)/6-31G(d,p) and HF/6-31G(d) level of theory, respectively.

2. Entropies and Heat Capacities. $S°_{298}$ and $C_p(T)$'s based on MP2(full)/6-31G(d,p) determined frequencies and geometry are summarized in Table 5. TVR, represents the sum of the contributions from translations, external rotations and vibrations for $S°_{298}$ and $C_p(T)$'s. Symmetry is incorporated in estimation of $S°_{298}$ as described in Table 5. The internal rotational contribution to $S°_{298}$ and $C_p(T)$'s is lost in the cyclic structure of TS1. This results in a lower $S°_{298}$ (ca. 6.9 cal/mol K) and $C_p(T)$'s (ca. 3.0 cal/mol K at 300 K) than the reactant. $S°_{298}$ increases by 1.5 and 0.2 cal/mol K in TS2 and TS3, respectively, relative to CH3CH2O·. $S°_{298}$ decreases by −1.78 cal/mol K in TS4 relative to C·H$_2$CH$_2$OH.

Table 6 lists $S°_{298}$ and $C_p(T)$ calculations using frequencies determined by HF/6-31G(d) level of calculation and geometries determined by MP2(full)/6-31G(d) level of calculation. These $S°_{298}$'s and $C_p(T)$'s are consistently higher (ca. 0.4 to 1.0 cal/mol K) than MP2(full)/6-31G(d,p) determined values.

3. Estimation of the Enthalpies of Formation. CBS-q determined enthalpy of reaction 1 ($\Delta H_{rxn}°_{298}$) is 0.43 kcal/mol. This near zero value of the calculated $\Delta H_{rxn}°_{298}$ supports our estimation of similar bonding environments for reaction. $\Delta H_f°_{298}$(C·H$_2$CH$_2$OH) is evaluated from $\Delta H_{rxn}°_{298} = \Delta H_f°_{298}$(C$_2H_5$OH) + $\Delta H_f°_{298}$(C$_2$H$_5$) − $\Delta H_f°_{298}$(C·H$_2$CH$_2$OH) − $\Delta H_f°_{298}$(C$_2$H$_6$)

$$0.43 = -56.12 + 28.32 - X - (-20.24)\ \text{kcal/mol} \quad (4)$$

The $\Delta H_f°_{298}$ of C·H$_2$CH$_2$OH obtained is −7.99 kcal/mol. This enthalpy of reaction $\Delta H_{rxn}°_{298}$) is also expressed using the calculated reaction energy: $\Delta H_{rxn}°_{298}$ = BDE(H−CH$_2$CH$_3$) − BDE(H−CH$_2$CH$_2$OH) = 0.43 kcal/mol.

Since BDE(H−CH$_2$CH$_3$) (BDE = bond dissociation energy) is known to be 101.6 kcal/mol, one can estimate BDE(H−CH$_2$-CH$_2$OH) as 101.2 kcal/mol.

Sosa et al. estimated $\Delta H_f°_0$ for C·H$_2$CH$_2$OH as −5.1 kcal/mol. They used frequencies and zero-point energies calculated by HF/3-21G* level of theory and geometries optimized by HF/6-31G* level of theory.[8] Their total energies at the highest level were estimated by adding the correction for spin contamination (PMP4/6-31G* − MP4/6-31G*) and for zero-point energies to the MP4/6-31G** energies.

$\Delta H_f°_{298}$ for the other intermediate radical, CH$_3$CH$_2$O·, is calculated using CBS-q and G2 determined energies and the isodesmic reaction 2. The resulting enthalpy values are −1.68 and −3.34 kcal/mol, respectively. Sosa et al. estimated the energy of CH$_3$CH$_2$O· relative to C$_2$H$_4$ + OH as −25.3 kcal/mol at 0 K[8]; our estimation is −23.7 kcal/mol at 298 K.

In the case of C$_2$H$_3$OH CBS-APNO (atomic pair natural orbital method) and G2, results are −29.95 and −29.46 kcal/

TABLE 5: Ideal Gas Phase Thermodynamic Properties Using CBS-q//MP2/6-31G(d,p)[a]

species and symmetry #		$H_f°_{298}$	$S°_{298}$[b]	C_{p300}[b]	C_{p400}	C_{p500}	C_{p600}	C_{p800}	C_{p1000}	C_{p1500}
C·H_2CH_2OH	TVR[c,d]		60.07	12.59	15.49	18.23	20.62	24.42	27.32	32.12
2	internal rotor[e]		7.94	3.07	3.04	2.96	2.86	2.65	2.49	2.26
	total	−7.99	69.39[f]	15.66	18.53	21.19	23.48	27.07	29.81	34.38
C·H_2CH_2OH	TVR		61.08	12.60	16.10	19.38	22.19	26.55	29.74	34.68
(TS1)[g]	internal rotor		0	0	0	0	0	0	0	0
2	total	21.78	62.46[f]	12.60	16.10	19.38	22.19	26.55	29.74	34.68
CH_3CH_2O·	TVR		58.99	12.24	15.36	18.4	21.09	25.43	28.73	33.99
3	internal rotor		3.99	2.04	2.19	2.17	2.07	1.82	1.62	1.34
	total	−1.68	64.36[f]	14.28	17.55	20.57	23.16	27.25	30.35	35.33
CH_3−CH_2O·	TVR		60.48	13.34	16.09	18.63	20.87	24.58	27.5	32.33
(TS2)[g]	internal rotor		3.99	2.04	2.19	2.17	2.07	1.82	1.62	1.34
3	total	11.67	65.85[f]	15.38	18.28	20.8	22.94	26.4	29.12	33.67
CH_3CHO−H	TVR		59.17	13.02	16.14	19.03	21.54	25.55	28.53	33.17
(TS3)[g]	internal rotor		3.99	2.05	2.19	2.17	2.07	1.83	1.62	1.34
3	total	15.92	64.54[f]	15.07	18.33	21.2	23.61	27.38	30.15	34.51
C_2H_3OH−H	TVR		62.22	16.29	19.91	22.89	25.28	28.84	31.42	35.51
(TS4)[g]	internal rotor		4.01	1.39	1.27	1.2	1.15	1.09	1.06	1.02
2	total	26.19	67.61[f]	17.68	21.18	24.09	26.43	29.93	32.48	36.53
C_2H_3OH	TVR		59.88	13.77	16.93	19.62	21.82	25.17	27.64	31.64
	internal rotor		0	0	0	0	0	0	0	0
2	total	−34.60[b] (−29.95)	59.88	13.77	16.93	19.62	21.82	25.17	27.64	31.64

[a] Thermodynamic properties are referred to a standard state of an ideal gas of pure enantiomeer at 1 atm. [b] In cal/mol K. [c] The sum of contributions from translations, external rotations, and vibrations. [d] Symmetry number is taken into account (−1.987ln(number of symmetry)). [e] Contribution from internal rotation. [f] Spin degeneracy contribution for entropy = 1.987ln(2) (cal/mol K) is taken into account. [g] TS structure described in Method section. [h] Number in parenthesis is CBS-APNO calculation result.

TABLE 6: Ideal Gas Phase Thermodynamic Properties Using G2[a]

species and symmetry no.		$H_f°_{298}$	$S°_{298}$[b]	C_{p300}[b]	C_{p400}	C_{p500}	C_{p600}	C_{p800}	C_{p1000}	C_{p1500}
C·H_2CH_2OH	TVR[c,d]		60.48	13.24	16.3	19.12	21.55	25.41	28.32	32.97
2	internal rotor[e]		7.94	3.07	3.04	2.96	2.86	2.65	2.49	2.26
	total	−5.99	69.80[f]	16.31	19.34	22.08	24.41	28.06	30.81	35.23
C·H_2CH_2OH	TVR		61.57	13.59	17.37	20.76	23.6	27.64	31.04	35.65
(TS1)[g]	internal rotor		0	0	0	0	0	0	0	0
2	total	24.83	62.95[f]	13.59	17.37	20.76	23.6	27.64	31.04	35.65
CH_3CH_2O·	TVR		59.87	13.46	16.69	19.75	22.43	26.77	30.02	35.01
3	internal rotor		3.99	2.04	2.19	2.17	2.07	1.82	1.62	1.34
	total	−3.34	65.24[f]	15.5	18.88	21.92	24.5	28.59	31.64	36.35
CH_3−CH_2O·	TVR		61.32	14.44	17.44	20.08	22.35	26.02	28.85	33.35
(TS2)	internal rotor		3.99	2.04	2.19	2.17	2.07	1.82	1.62	1.34
3	total	12.7	66.69[f]	16.48	19.63	22.25	24.42	27.84	30.47	34.69
CH_3CHO−H	TVR		59.89	14.07	13.93	17.45	20.51	23.19	27.11	30.06
(TS3)	internal rotor		3.99	2.05	2.19	2.17	2.07	1.83	1.62	1.34
3	total	15.88	65.26[f]	16.12	19.62	22.58	25.02	28.73	31.4	35.42
C_2H_3OH−H	TVR		63.29	17.47	21.04	23.91	26.19	29.59	32.06	35.96
(TS4)	internal rotor		4.01	1.39	1.27	1.2	1.15	1.09	1.06	1.02
2	total	25.99	68.68[f]	18.86	22.31	25.11	27.34	30.68	33.12	36.98
C_2H_3OH	TVR		59.86	13.68	16.84	19.56	21.81	25.27	27.81	31.84
	internal rotor		0	0	0	0	0	0	0	0
2	total	−29.46	59.86	13.68	16.84	19.56	21.81	25.27	27.81	31.84

[a] Thermodynamic properties are referred to a standard state of an ideal gas of pure enantiomeer at 1 atm. [b] In cal/mol K. [c] The sum of contributions from translations, external rotations, and vibrations. [d] Symmetry number is taken into account (−1.987ln(number of symmetry)). [e] Contribution from internal rotation. [f] Spin degeneracy contribution for entropy = 1.987ln(2) (cal/mol K) is taken into account. [g] TS structure described in Method section.

TABLE 7: Molecules Considered to Have Known $\Delta H_f°_{298}$ for Use in Isodesmic Reactions

compounds	$\Delta H_f°_{298}$ (kcal/mol)
C_2H_6	−20.24[a]
C_2H_5OH	−56.12[a]
C_2H_5	28.32[b]
CH_3OH	−48.08[a]
CH_3O	4.00[b]
C_2H_4	12.50[a]

[a] Reference 33. [b] Reference 49.

mol, respectively. CBS-q/mp2/6-31G(d.p) calculation shows unreasonably low energy, −34.60 kcal/mol, and a higher level calculation CBS-APNO is performed. APNO uses frequencies of HF/6-311G(d,p) level, the optimized geometry of the QCISD(T)/6-311G(d,p) level, and higher order correlation energy via the QCISD(T)/6-311++G(2df,p) as well as SCF and MP2 energies.[43] Turecek et al. reported the $\Delta H_f°_{298}$ of vinyl alcohol as −29.6 kcal/mol using G2(MP2) determined total energy and same isodesmic reaction as our study.[44] Sosa et al. estimated relative energy of C_2H_3OH + H to C_2H_4 + OH as 5.5 kcal/mol,[8] while our value is 0.15 kcal /mol using CBS-APNO determined $\Delta H_f°_{298}$ of C_2H_3OH. Smith et al. calculated energy of CH_2CHOH relative to acetaldehyde using G1; their result is 11.23 kcal/mol above acetaldehyde,[9] which places $\Delta H_f°_{298}$ of vinyl alcohol at −28.53 kcal/mol. Espinosa has performed ab initio calculations at several high levels of theory

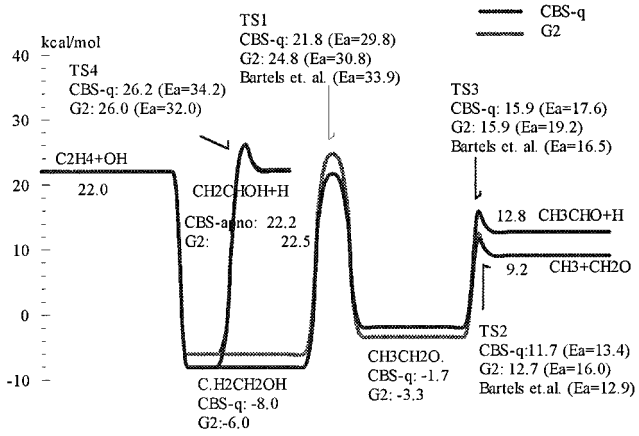

Figure 7. Potential energy diagram determined by CBS-q//MP2(full)/6-31G(d,p) and G2.

and used different isodesmic reaction to evaluate $\Delta H_f°_{298}$ of the C·H_2CH_2OH radical.[45] Their reported value is -4.0 ± 1.0 kcal/mol, 4 kcal/mol higher than the vlaue determined and used in this study. We feel their calculations are of value and do not know why such a large difference exists. The -4.0 kcal/mol value of Espinosa combined with a $\Delta H_f°_{298}$ of -56.2 kcal/mol for ethanol places the C−H bond energy of the methyl group on ethanol at 104.3 kcal/mol. We look to further studies to clarify this value.

The activation energy of TS1 is estimated from the both reactant C·H_2CH_2OH and product CH_3CH_2O· sides. The averaged results are 29.77 and 30.82 kcal/mol for the CBS-q and G2 calculation respectively. Sosa et al. estimated E_a for TS1 as 31.9 kcal/mol using spin contamination annihilation.[8] The activation energies of TS2, TS3, and TS4 are estimated by taking the difference of total energy between transition state and reactant, resulting in 13.35, 17.60, and 34.2 kcal/mol respectively with the CBS-q calculation and 16.04, 19.22, and 31.98 kcal/mol respectively with the G2 calculation. Sosa et al. estimated these values as 18.2, 22.4, and 34.0 kcal/mol, respectively, where TS3 and TS4 were estimated from reverse directions ($CH_3CHO + H \rightarrow CH_3CH_2O$· for TS3 and $C_2H_3OH + H \rightarrow$ C·H_2CH_2OH for TS4).[8] $\Delta H_f°_{298}$ using our CBS-q composite calculations are listed in Table 5: G2 values are listed in Table 6. The overall energy diagram for the reaction system is illustrated in Figure 7.

4. Tunneling Consideration and Imaginary Frequency Adjustment. The direct use of ab initio determined thermodynamic properties for QRRK analysis shows good agreement of overall forward rate constant $k_{\infty,f}$ with experimental data at the temperatures of 296 and 524 K.[6] A large difference exists, however, in the branching ratio to products (C·H_2CH_2OH:$CH_2O + CH_3$:$CH_3CHO + H$) at 2 torr and 295 K with the experimental data of Bartels et al.[12] The experimentally determined branching ratio is: (C·H_2CH_2OH stabilization:$CH_2O + CH_3$:$CH_3CHO + H$) = (21:44:35 = 1:2.1:1.7), where the QRRK calculation with CBS-q and G2 results in (1:2.0) $\times 10^{-2}$:8.2 $\times 10^{-4}$ and (1:1.9) $\times 10^{-4}$:4.8 $\times 10^{-6}$, respectively.

Our first attempt to match the experimental data involved lowering activation energies for TS1 and TS3. A match of branching ratio with experimental data between the adduct C·H_2CH_2OH and one product set $CH_2O + CH_3$ can be obtained by reducing the activation energy of TS1 by 4.2 kcal/mol. The experimental branching ratio for $CH_3CHO + H$ is not obtained even if the E_a of TS3 is decreased to the reaction endoergicity (12.8 kcal/mol), which indicates zero activation energy for the reverse (H addition) reaction ($CH_3CHO + H \rightarrow CH_3CH_2O$·).

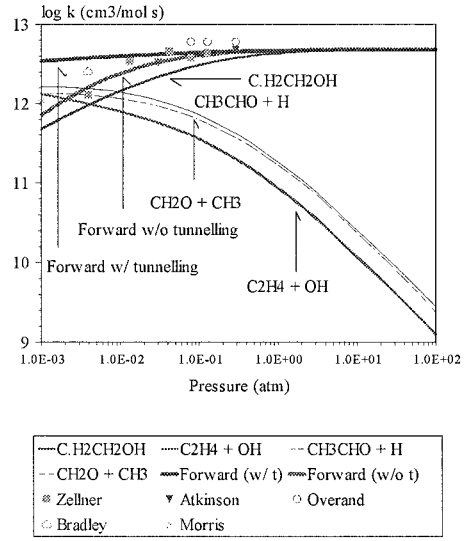

Figure 8. QRRK analysis results. Rate constant vs pressure at 296 K.

The best fit of branching ratio underestimates the CH_3CHO + H channel by a factor of 4 (C·H_2CH_2OH stabilization:CH_2O + CH_3:CH_3CHO + H) = (1:2.1:0.4). Reducing the activation energy of TS1 by 4.2 kcal/mol is unrealistic, even though part of the experimental data is matched. Tunneling is considered instead of decreasing activation energies; Sosa et al. also suggested that tunneling could be important.[8]

The imaginary frequencies for TS1 and TS3 based on MP2(full)/6-31G(d,p) optimized structure are 2344i and 1704i cm^{-1}, respectively, where HF/3-21G determined frequencies reported by Sosa et al. are 2599i and 805i cm^{-1}, respectively.[8] Direct use of this frequency derived by MP2(full)/6-31G(d,p) in the tunneling calculation results in the corrections of 7.84 $\times 10^6$, 1.68 $\times 10^5$, and 5.25 $\times 10^3$ for TS1 forward, TS1 reverse, and TS3 forward directions, respectively, at 295 K; we consider these corrections excessive.

The imaginary (TST reaction coordinate) frequencies are adjusted as -1580 and -550 cm^{-1} for TS1 and TS3, respectively. The calculated tunneling correction factors (Γ*) correspond to these frequencies at 295 K are 824 for the TS1 forward direction, 93 for the TS1 reverse direction, and 21 for the TS3 forward direction. These values are convoluted into the corresponding A_∞ factors. The QRRK analysis performed at 295 K and 2 torr results in the branching ratio obtained by Bartels et al.[12]: 1:2.1:1.7. William et al. applied tunneling effect into their ab initio study of transition state for $C_2H_5 \leftrightarrow H + C_2H_4$.[46] Their calculated activation energy and imaginary frequency were 3.5 kcal/mol and 860.0 cm^{-1} using QCISD/6-311+G(2df,p). The activation energy and imaginary frequency were adjusted until the experimental rate constant was fit; their result is E_a of 2.00 kcal/mol and an imaginary frequency of 710 cm^{-1}.[46] Schwartz et al. note that calculated vibrational frequencies using HF/6-31G(d) level of theory need to be reduced by one-half to one-third in order for calculated transition states rate constant to match experimental data in abstraction reactions from Fluorinated methanes.[47]

5. QRRK Analysis Results. QRRK analysis is performed at the temperatures of 290, 296, 325, 400, 524, 700, 900, and 1200 K. Results are shown in Figures 8 and 9 for rate constants to specific products versus pressure at 296 and 524 K, respectively, while Figure 10 illustrates the rate constants to specific products versus temperature at 1 atm. The H shift isomerization and H atom elimination A_∞ factors are multiplied by the corresponding tunneling contribution at each temperature.

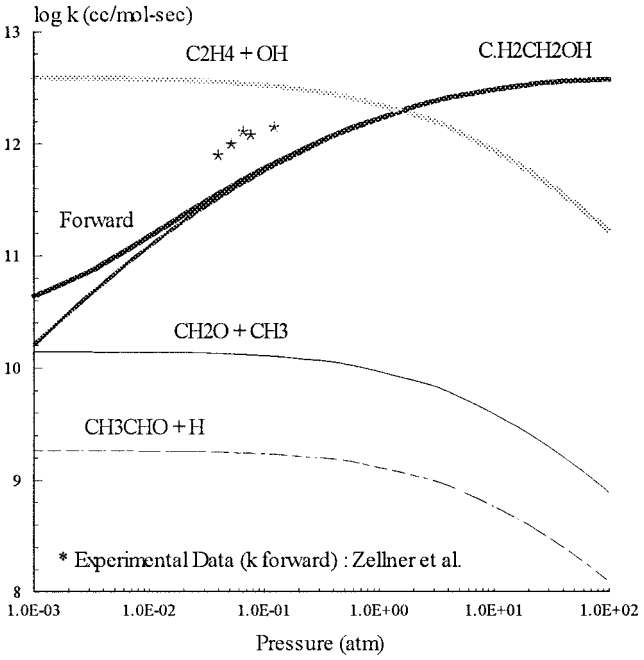

Figure 9. QRRK analysis results. Rate constant vs pressure at 524 K.

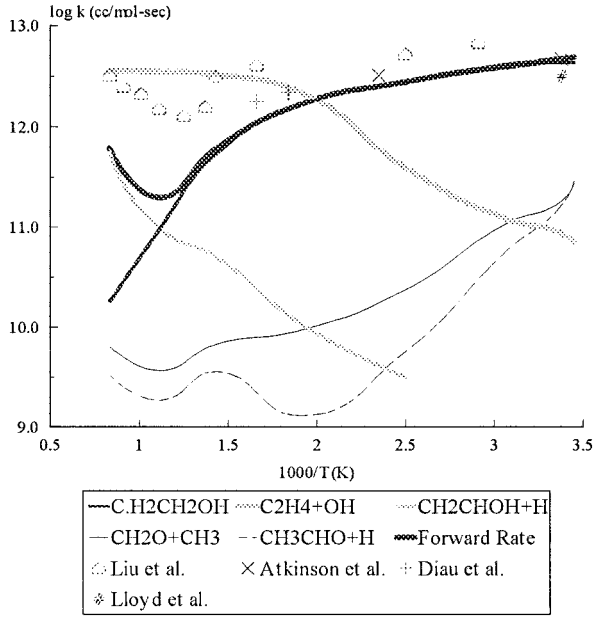

Figure 10. QRRK analysis results: rate constant vs temperature at 1 atm. Abstraction reactions are not included in the calculated data.

The quadratic form of the high-pressure limit rate constant ($k_{\infty,1}$) for C_2H_4 + OH, reported by Villa et al. is adopted;[7] both A_∞ and $E_{a,\infty}$ vary strongly with temperature. Monotonous trends in three temperature regions are used to represent their quadratic form. Arrhenius A factors (A(T)) are multiplied by 1.4 to match the high-pressure limit experimental data in the 290 to 450 K temperature range.[4,11,17,48] $A_{1,\infty}$ and $E_{a1,\infty}$ used in this study are 1.00×10^{12} cm^3/mol s and -0.92 kcal/mol respectively in the temperature range 290−450 K. $A_{1,\infty}$'s and $E_{a1,\infty}$'s in the temperature range 450−700 K and above 700 K are 3.89×10^{12} cm^3/mol s, 0.0 kcal/mol, and 6.19×10^{12} cm^3/mol s, 0.92 kcal/mol, respectively (see Table 9). Small negative temperature activation energies are reported in other low temperature studies: -0.9 ± 0.2 kcal/mol is reported by Greiner and Tully,[3,5] -0.7 ± 0.3 kcal/mol by Atkinson et al.,[4] and -0.6 ± 0.3 kcal/mol by Zellner et al.[6] Table 8 lists the QRRK input parameters for this reaction system at temperature of 296 K. Table 9 summarizes A_∞, E_a in each of the three temperature ranges and Γ* for TS1(forward), TS1(reverse), and TS3(forward) at each temperature used in QRRK analysis.

TABLE 8: Input Parameters[a] and High-Pressure Limit Rate Constants (k_∞)[b] for QRRK Calculations[c] (Temp = 296K): CBS-q Result

		k_∞		
	reaction	A(S^{-1} or cm^3/(mol s))	n	E_a (kcal/mol)
1	$C_2H_4 + OH \rightleftharpoons C{\cdot}H_2CH_2OH$[d]	see text, Table 9		
−1	$C{\cdot}H_2CH_2OH \rightleftharpoons C_2H_4 + OH$[e]			
2	$C{\cdot}H_2CH_2OH \rightleftharpoons C_2H_3OH + H$[f]	2.16×10^5	2.84	32.92
3	$C{\cdot}H_2CH_2OH \rightleftharpoons CH_3CH_2O$[g]	4.54×10^{12}	0.60	29.77
−3	$CH_3CH_2O \rightleftharpoons C{\cdot}H_2CH_2OH$[h]	1.23×10^{13}	0.56	23.47
4	$CH_3CH_2O \rightleftharpoons CH_2O + CH_3$[i]	5.90×10^{11}	0.67	13.63
5	$CH_3CH_2O \rightleftharpoons CH_3CHO + H$[j]	3.64×10^{11}	1.07	17.58

[a] Geometric mean frequency (from CPFIT, ref 50: 401.1 cm^{-1} (4.446), 1312.0 cm^{-1} (7.795), 3415.6 cm^{-1} (4.760). Lennard-Jones parameters: $\sigma_{ij} = 4.35$Å, $(\epsilon/k = 423$. [b] The units of A factors and rate constants k are s^{-1} for unimolecular reactions and cm^3/(mol s) for bimolecular reactions. [c] ΔE down of 400 cal/mol is used. [d] $k_{\infty,1}$, Villa et al. [e] $k_{\infty,-1}$, MR. [f] A_2 is calculated using TST and entropy of transition state (TS4), ($S^{\neq}_{298}$ from MP2(full)/6-31G(d,p) (see Table 5), E_a from CBS-q calculation (see Table 5 and description for determination of E_a in Results section). [g] A_3 is calculated using TST and entropy of transition state (TS1), tunneling correction = 842 is taken into account, $\Delta S^{\neq}_{298}$ from MP2(full)/6-31G(d,p) (see Table 5), E_a from CBS-q calculation (see Table 5 and description for determination of E_a in Results section). [h] A_{-3} is calculated using TST and entropy of transition state (TS1), tunneling correction = 93.1 is taken into account, ($S^{\neq}_{298}$ from MP2(full)/6-31G(d,p) (see Table 5), E_a from CBS-q calculation (see Table 5 and description for determination of E_a in Results section). [i] A_4 is calculated using TST and entropy of transition state (TS2), ($S^{\neq}_{298}$ from MP2(full)/6-31G(d,p) (see Table 5), E_a from CBS-q calculation (see Table 5 and description for determination of E_a in Results section). [j] A_5 is calculated using TST and entropy of transition state (TS3), tunneling correction = 21.1, ($S^{\neq}_{298}$ from MP2(full)/6-31G(d,p) (see Table 5), E_a from CBS-q calculation (see Table 5 and description for determination of E_a in Results section).

TABLE 9: Variables (A_1, $E_{a,1}$ and Γ* for TS1(Forward), TS1(Reverse), and TS3(Forward)

temperature (K)	A_1	$E_{a,1}$	Γ* TS1-(forward)	Γ* TS1-(reverse)	Γ* TS3-(forward)
290	1.00×10^{12}	−0.92	1.39×10^3	1.31×10^2	2.46×10^1
296	1.00×10^{12}	−0.92	8.42×10^2	9.31×10^1	2.11×10^1
325	1.00×10^{12}	−0.92	1.26×10^2	2.70×10^1	1.13×10^1
400	1.00×10^{12}	−0.92	1.15×10^1	5.90×10	4.33×10
524	3.89×10^{12}	0.00	3.27×10	2.49×10	2.21×10
700	3.89×10^{12}	0.00	1.85×10	1.62×10	1.53×10
900	6.19×10^{12}	0.92	1.44×10	1.34×10	1.29×10
1200	6.19×10^{12}	0.92	1.23×10	1.18×10	1.16×10

Figure 8 and 9 show QRRK analysis rate constant results vs. pressure 0.001 to 100 atm at 296 and 524 K, respectively. The calculation at 296 K for the overall forward rate constant shows higher values below 0.01 atm than Zellner et al.'s experimental data,[6] and does not show significant falloff, while the total forward rate constant without tunneling slightly underestimates the data of Zellner et al.[6], but does show fall off. This loss of falloff behavior is due to increased rate constants k_2, $C{\cdot}H_2CH_2$-$OH \rightarrow CH_3CH_2O^{\bullet}$, and k_5, $CH_3CH_2O^{\bullet} \rightarrow CH_3CHO + H$ resulting from tunneling. The rate constants k_4, $CH_2O + CH_3$, and k_5, $CH_3CHO + H$, are similar over the entire pressure range at 296 K. These reactions are important at pressure below 0.01 atm where experiments on elementary reactions are often performed. The stabilization reaction to ethylene-OH adduct dominates the reaction at pressures above 0.01 atm. The

agreement of our QRRK/falloff analysis with experimental data over a wide pressure and temperature range illustrates its value.

The QRRK analysis at 524 K and of 0.001−100 atm. slightly underestimates the overall reaction rate compared with experimental data.[6] The dissociation back to reactants dominates at pressure below 2 atm, and stabilization to ethylene−OH adduct dominates at high pressure.

Figure 10 shows k vs temperature at 1 atm. Smooth curves are not obtained because inclusion of tunneling requires different input values for A_∞ and $E_{a,\infty}$ of TS1 and TS3 at each temperature in the $C_2H_4 + OH \rightarrow C{\cdot}H_2CH_2OH$ system. Stabilization to form ethylene-OH adduct is major reaction at temperature up to 500 K. Energized adduct dissociation back to reactants is the major reaction at temperature above 500 K. The calculated and experimentally determined literature value for forward rate constants are also shown in Figure 10. The calculated forward rate constant shows falloff up to temperature of 900 K, then increases with temperature due to the increasing rate constant for $C_2H_4 + OH \rightarrow CH_2CHOH + H$ at high temperature. While our calculation underestimates the forward rate constant compared with Liu et al.'s experimental data;[2] their results include the abstraction channel $C_2H_4 + OH \rightarrow C_2H_3 + H_2O$, which is not included in our calculation. The lack of importance of the two aldehyde channels at 1 atm and higher temperatures is due to the tightness (lower entropy) of the TS1 transition state structure, relative to the elimination transition states and the increased importance of stabilization.

Summary

Thermodynamic properties of stable radicals and transition states are calculated on the $C_2H_4 + OH$ addition reaction system using composite ab initio methods; CBS-q//MP2(full)/6-31G(d,p) and G2. Data from the CBS-q and G2 levels of theory show good agreement. $H_f°_{298}$ for the stable radicals $C{\cdot}H_2CH_2$-OH and $CH_3CH_2O^{\bullet}$ are estimated using total energies derived from CBS-q and G2 calculations and isodesmic reactions with ZPVE and thermal correction to 298.15 K. $H_f°_{298}$ for CH_2CHOH is estimated using CBS-APNO and G2. QRRK analysis is used for $k(E)$ and master equation analysis is used for falloff to estimate kinetic parameters as a function of pressure and temperature. Tunneling is incorporated in transition states TS1 and TS3, where H shift and H atom elimination reactions occur. The imaginary frequencies, which play an important role in the tunneling calculation, are adjusted to fit the experimental branching ratio. Tunneling corrections to rate constants at 296 K are 842, 93, and 21 for TS1 forward, TS1 reverse, and TS3 forward directions, respectively. Rate constants for adduct formation, $C_2H_4 + OH \rightarrow C{\cdot}H_2CH_2OH$, use the quadratic form of k vs T from Villa et al.'s canonical variational TST analysis. Overall rate constants for OH addition to ethylene and branching ratio ($C{\cdot}H_2CH_2OH$ stabilization: CH_2O+CH_3, CH_3CHO+H) at 2 torr and 295 K based on CBS-q//MP2(full)/6-31G(d,p) values and QRRK calculations compare well with experimental results. Chemical activation and falloff are of major importance in determination of dominant reaction paths and rate constants as functions of pressure and temperature in this $C_2H_4 + OH$ system.

References and Notes

(1) Sosa, C.; Schlegel, H. B. *J. Am. Chem. Soc.* **1987**, *109*, 4193.
(2) Liu, A.; Mulac, W. A.; Jonah, C. D. *J. Phys. Chem.* **1988**, *92*, 3828.
(3) Griener, N. R. *J. Chem. Phys.* **1970**, *53*, 1284.
(4) Atkinson, R.; Perry, R. A.; Pitts, J. N. *J. Chem. Phys.* **1977**, *66*, 1197.
(5) Tully, F. P. *Chem. Phys. Lett.* **1983**, *96*, 148.
(6) Zellner, R.; Lorenz, K. *J. Phys. Chem.* **1984**, *88*, 984.
(7) Villa, J.; Gonzalez-Lafont, A.; Lluch, J. M.; Corchado, J. C.; Espinosa-Garcia, J. *J. Chem. Phys.* **1997**, *107*, 7266.
(8) Sosa, C.; Schlegel, H. B. *J. Am. Chem. Soc.* **1986**, *109*, 7007.
(9) Smith, B. J.; Nguyen, M. T.; Bouma, W. J.; Radom, L. *J. Am. Chem. Soc.* **1991**, *113*, 6452.
(10) Meagher, J. F.; Heicklen, J. *J. Phys. Chem.* **1976**, *80*, 1645.
(11) Lloyd, A. C.; Darnall, K. R.; Winer, A. M.; Pitts, J. M. *J. Phys. Chem.* **1976**, *80*, 789.
(12) Bartels, M.; Hoyermann, K.; Sievert, R. Elementary Reactions in the Oxidation of Etylene. Presented at the International Symposium (Int.) Combustion, 1982, Napoli, Italy.
(13) Liu, A.; Jonah, C. D.; Mulac, W. A. *Radiat. Phys. Chem.* **1989**, *34*, 687.
(14) Smith, I. W. M.; Zellner, R. *J. Chem. Soc., Faraday Trans. 2* **1973**, *69*, 1617.
(15) Mozurkewich, M.; Benson, S. W. *J. Phys. Chem.* **1984**, *88*, 6429.
(16) Howard, C. J. *J. Chem. Phys.* **1976**, *65*, 4771.
(17) Diau, E. W.-G.; Lee, Y.-P. *J. Chem. Phys* **1992**, *96*, 377.
(18) Pastrana, A. V.; Carr, J. R. W. *J. Phys. Chem.* **1975**, *79*, 765.
(19) Morris, E. D.; Stedman, D. H.; Niki, H. *J. Am. Chem. Soc.* **1971**, *93*, 3570.
(20) Bradley, J. N.; Hack, W.; Hoyermann, K.; Wagner, H. G. *J. Chem. Soc., Faraday Trans. 1* **1973**, *69*, 1889.
(21) Kuo, C.-H.; Lee, Y.-P. *J. Phys. Chem.* **1991**, *95*, 1253.
(22) Overend, R.; Paraskevopoulos, G. *J. Chem. Phys.* **1977**, *67*, 674.
(23) Fulle, D.; Hamann, H. F.; Hippler, H.; Jansch, C. P. *Ber. Bunsen-Ges. Phys. Chem.* **1997**, *101*, 1433.
(24) Chang, A. M.; Bozzelli, J. W.; Dean, A. M. To be submitted.
(25) Ochterski, J. W.; Petersson, G. A.; Montgomery, J. J. A. *J. Chem. Phys.* **1996**, *104*, 2598.
(26) Curtiss, L. A.; Raghavachari, K.; Trucks, G. W.; Pople, J. H. *J. Chem. Phys.* **1991**, *94*, 7221.
(27) Frisch, M. J.; Trucks, G. W.; Schlegel, H. B.; Gill, P. M. W.; Johnson, B. G.; Robb, M. A.; Cheeseman, R. J.; Keith, T.; Petersson, G. A.; Montgomery, J. A.; Raghavachari, K.; Al-Laham, M. A.; Zakrzewski, V. G.; Ortiz, J. V.; Foresman, J. B.; Cioslowski, J.; Stefanov, B. B.; Nanayakkara, A.; Challacombe, M.; Peng, C. Y.; Ayala, P. Y.; Chen, W.; Wong, M. W.; Andres, J. L.; Replogle, E. S.; Gomperts, R.; Martin, R. L.; Fox, D. J.; Binkley, J. S.; Defrees, D. J.; Baker, J.; Stewart, J. P.; Head-Gordon, M.; Gonzalez, C.; Pople, J. A. *Gaussian 94*; Gaussian, Inc.: Pittsburgh, PA, 1995.
(28) Curtiss, L. A.; Raghavachari, K.; Pople, J. A. *J. Chem. Phys.* **1993**, *98*, 1293.
(29) Scott, A. P.; Radom, L. *J. Phys. Chem.* **1996**, *100*, 16502.
(30) Hehre, W. J.; Radom, L.; Schleyer, P. R.; Pople, J. A. *Ab Initio Molecular Orbital Theory*; John Wiley & Sons: New York, 1986; Chapter 6.
(31) Pitzer, K. S.; Gwinn, W. *J. Chem. Phys.* **1942**, *10*, 428.
(32) Stull, D. R.; Prophet, H. *JANAF Thermochemical Tables*; U.S. Government Printing Office: Washington DC, 1971; Vol. NSRDS-NBS 37.
(33) Stull, D. R.; Westrum, E. F.; Sinke, G. C. *The Chemical Thermodynamics of Organic Compounds*; Robert E. Krieger Publishing Company: Malabar, FL, 1987.
(34) Lay, T. H.; Krasnoperov, L. N.; Venanzi, C. A.; Bozzelli, J. W. *J. Phys. Chem.* **1996**, *100*, 8240.
(35) Benson, S. W. *Thermochemical Kinetics*; Wiley-Interscience Publishers: New York, 1976.
(36) Westmoreland, P. R. *Combust. Sci. Technol.* **1992**, *82*, 1515.
(37) Bozzelli, B. W.; Dean, A. M.; Ritter, E. R. *Combust. Sci. Technol.* **1991**, *80*, 169.
(38) Dean, A. M. *J. Phys. Chem.* **1985**, *89*, 4500.
(39) Gilbert, R. G.; Smith, S. C. *Theory of Unimolecular and Recombination Reactions*; Oxford Press: Boston, 1990.
(40) Gilbert, R. G.; Smith, C. S. UNIMOL, 1990.
(41) Petersson, G.; Schwartz, M. Personal Communication:.
(42) Eckart, C. *Phys. Rev.* **1930**, *35*, 1203.
(43) Montgomery, J. A.; Ochterski, J. W.; Petersson, G. A. *J. Phys. Chem.* **1994**, *101*, 5900.
(44) Turecek, F.; Cramer, C. J. *J. Am. Chem. Soc.* **1995**, *117*, 12243.
(45) Espinosa-Garcia, J. *Chem. Phys. Lett.* **1997**, *278*, 209.
(46) William, L. H.; Schlegel, H. B.; Balbyshev, V.; Page, M. *J. Phys. Chem.* **1996**, *100*, 5354.
(47) Schwartz, M.; Marshall, P.; Berry, R. J.; Ehlers, C. J.; Petersson, G. A. *J. Phys. Chem.* **1998**, *102*, 10074.
(48) Liu, A.-D.; Mulac, W. I.; Jonah, C. D. *Int. J. Chem. Kinet.* **1987**, *19*, 25.
(49) Tsang, W.; Hampson, R. F. *J. Phys. Chem. Ref. Data* **1986**, *15*, 1087.
(50) Bozzelli, J. W.; Chang, A. Y.; Dean, A. M. *Int. J. Chem. Kintet.* **1997**, *29*, 161.
(51) Orlando, J.; Tyndall, G. S.; Bilde, M.; Ferronato, C., Wallington, T. J.; Vereeken, L.; Peeters, J. *J. Phys. Chem.* **1998**, *102*, 8116.